Table 1. Composition of samples used in preparing the dye-doped polymer-stabilized blue phases.

	Monomer		Photoinitiator	Liquid Crystal			Laser dye
	12A	RM257	DMPAP	JC-1041XX	5CB	ISO-(6OBA)$_2$	Py597
Weight ratio [wt.-%]	50	50		46.75	46.75	6.5	
Composite [wt.-%]	7.5		0.3		91.7		0.5

homogeneous mixture and irradiated with UV light (365 nm, L2859–01, Hamamatsu Photonics) of 1.5 mW cm^{-2} intensity. During photoirradiation, we monitored the optical texture of the blue phases with a polarizing optical microscope.

Optical experiments were conducted with an optical microscope (IX71, Olympus) combined with spectrometers (USB2000, Ocean Optics). We focused the non-polarized white-light beam from a tungsten halogen light source (L7893, Hamamatsu Photonics) on the surface of the sample with a spot size of 30 μm in diameter through an objective ($\times$50, LC Plan Apo, Olympus). The spontaneous emission spectra from the blue phases were measured by using a continuous-wave (CW) laser (532 nm, 0.13 mW, Edmund Optics), and lasing spectra were measured by a Q-switched Nd:YAG (yttrium aluminum garnet) laser (532 nm, 8 ns pulse, Polaris II, New Wave Research). The excitation energy was adjusted using a half-wave plate in combination with a polarizing prism. The excitation beam was conducted to the optical microscope and focused onto the sample surface through an objective ($\times$20, LC Plan Apo, Olympus) to obtain a spot size of about 50 μm. We collected the laser emission from the sample in transmission and analyzed the spectrum with a spectrometer (Spectra Pro. 150 and charge-coupled device (CCD) detector 256HB, Acton Research).

Received: July 1, 2005
Final version: September 13, 2005
Published online: December 5, 2005

[1] E. Yablonovitch, *Phys. Rev. Lett.* **1987**, *58*, 2059.
[2] M. Imada, S. Noda, A. Chutinan, T. Tokuda, M. Murata, G. Sasaki, *Appl. Phys. Lett.* **1999**, *75*, 316.
[3] O. Painter, R. K. Lee, A. Scherer, A. Yariv, J. D. O'Brien, P. D. Papkus, I. Kim, *Science* **1999**, *284*, 1819.
[4] M. Loncar, T. Yoshie, A. Scherer, P. Gogna, Y. Qiu, *Appl. Phys. Lett.* **2002**, *81*, 2680.
[5] H. Coles, in *Handbook of Liquid Crystals* (Eds: D. Demus, J. Goodby, G. W. Gray, H.-W. Spiess, V. Vill), Vol. 2A, Wiley-VCH, Weinheim, Germany **1998**, pp. 335–409.
[6] H. Finkelmann, S. T. Kim, A. Muñoz, P. Palffy-Muhoray, B. Taheri, *Adv. Mater.* **2001**, *14*, 1069.
[7] S. Furumi, S. Yokoyama, A. Otomo, S. Mashiko, *Appl. Phys. Lett.* **2003**, *82*, 16.
[8] M. Ozaki, M. Kasano, D. Ganzke, W. Hasse, K. Yoshino, *Adv. Mater.* **2002**, *14*, 306.
[9] J. Schmidtke, W. Stille, H. Finkelmann, *Phys. Rev. Lett.* **2003**, *90*, 083 902.
[10] M. H. Song, B. Park, K. Shin, T. Ohta, Y. Tsunoda, H. Hoshi, Y. Takanishi, K. Ishikawa, J. Watanabe, S. Nishimura, T. Toyooka, Z. Zhu, T. M. Swager, H. Takezoe, *Adv. Mater.* **2004**, *16*, 779.
[11] Y. Matsuhisa, R. Ozaki, M. Ozaki, K. Yoshino, *Jpn. J. Appl. Phys., Part 2* **2005**, *44*, L629.
[12] P. P. Crooker, *Liq. Cryst.* **1989**, *5*, 751.
[13] R. M. Hornreich, S. Shtrikman, C. Sommers, *Phys. Rev. E* **1993**, *47*, 2067.
[14] D. L. Johnson, J. H. Flack, P. P. Crooker, *Phys. Rev. Lett.* **1980**, *45*, 641.
[15] W. Cao, A. Muñoz, P. Palffy-Muhoray, B. Taheri, *Nat. Mater.* **2002**, *1*, 111.
[16] H. Kikuchi, M. Yokota, Y. Hisakado, H. Yang, T. Kajiyama, *Nat. Mater.* **2002**, *1*, 64.
[17] H. J. Coles, M. N. Pivnenko, *Nature* **2005**, *436*, 997.
[18] S. Meiboom, M. Sammon, *Phys. Rev. Lett.* **1980**, *44*, 882.
[19] T. Matsui, R. Ozaki, K. Funamoto, M. Ozaki, K. Yoshino, *Appl. Phys. Lett.* **2002**, *81*, 3741.
[20] K. Uchida, Y. Hisakado, H. Kikuchi, T. Kajiyama, *Trans. Mater. Res. Soc. Jpn.* **2004**, *29*, 819.

DOI: 10.1002/adma.200501138

Multicolor Photoluminescence from Porous Silicon Using Focused, High-Energy Helium Ions**

By *Ee Jin Teo*,* *Mark B. H. Breese*, *Andrew A. Bettiol*, *Dharmalingam Mangaiyarkarasi*, *Frederic Champeaux*, *Frank Watt*, and *Daniel J. Blackwood*

Bulk silicon is a poor emitter of light owing to its indirect bandgap, which has greatly limited its integration in optoelectronic and photonic devices. Consequently there have been great efforts in the last decade to produce controlled light emission from silicon in the near-infrared and visible regions with silicon/silicon dioxide superlattices,[1] silicon nanocrystals in silicon dioxide,[2–4] and porous silicon.

Porous silicon is typically produced by electrochemical anodization of a silicon wafer in a hydrofluoric acid electrolyte.[5] The electrical-hole current flowing to the wafer surface facilitates a reaction with the electrolyte, leading to partial dissolution of the silicon surface. This results in a highly porous silicon skeleton from which red–orange photoluminescence (PL) is observed, which is commonly attributed to quantum-con-

[*] Dr. E. J. Teo, Prof. M. B. H. Breese, Dr. A. A. Bettiol, Dr. D. Mangaiyarkarasi, F. Champeaux, Prof. F. Watt
Department of Physics, Centre for Ion Beam Applications
National University of Singapore
2 Science Drive 3, Singapore 117542 (Singapore)
E-mail: msetej@nus.edu.sg
Dr. E. J. Teo, Prof. D. Blackwood
Department of Materials Science & Engineering
National University of Singapore
Singapore 117542 (Singapore)

[**] This work has been supported by the Agency for Science, Technology and Research (ASTAR) in Singapore.

ADVANCED MATERIALS

finement effects due to the low dimensionality of the remaining silicon islands.[6–9] This raises the possibility of producing porous-silicon light-emitting devices which are compatible with microelectronics technology,[10] and combined optical and electronic devices,[11] incorporating patterned, porous material directly onto a single-crystal substrate.

Many demonstrations of patterning porous silicon have shown selective quenching or enhancement of PL intensity by using a variety of optical,[12] photolithographic,[13] electron,[14] soft-lithography,[15] and ion-irradiation methods.[16–18] However, attempts to produce patterned areas with widely differing emission wavelengths using light or electron beams have failed because such irradiation only alters the rate of anodization, not the properties of the silicon wafer. In contrast, ion irradiation alters the resistivity of the silicon, which affects the wavelength emission in addition to its intensity. This effect has been observed using low doses of 100–300 keV Si-ion irradiation.[16,19] In this work, we employ 2 MeV helium ions to pre-irradiate the silicon instead of the lower-energy, heavier ions used in previous studies. According to SRIM calculations,[20] the damage created is 2–3 orders of magnitude lower than that of 300 keV Si ions, and extends to a depth of 7 μm rather than 400 nm. This provides greater control over the resultant PL emission due to the thicker damaged layer and reduced rate of damage with each dose. We use this principle to produce patterned, micrometer-sized areas of porous silicon with widely differing PL wavelengths and intensities on a single substrate, and explain these results in terms of the ion-induced changes in the wafer resistivity.

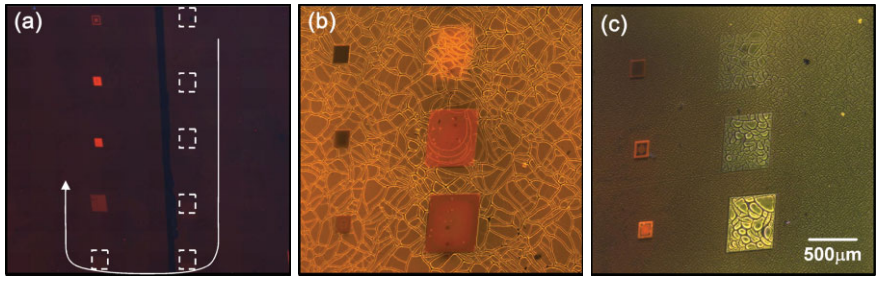

Figure 1. PL images of a) 0.02, b) 0.3, and c) 3 Ω cm resistivity p-type silicon wafers irradiated with a range of doses. The arrow points in the direction of increasing dose for all three images. a) Square patterns irradiated with doses of 5×10^{12}, 1×10^{13}, 2×10^{13}, 5×10^{13}, up to 5×10^{15} cm^{-2}. The locations of lower doses irradiation are outlined by dotted squares, since no visible PL is produced. In (b) and (c), irradiations of 5×10^{11}, 1×10^{12}, 2×10^{12}, 5×10^{12}, up to 2×10^{13} cm^{-2} are displayed.

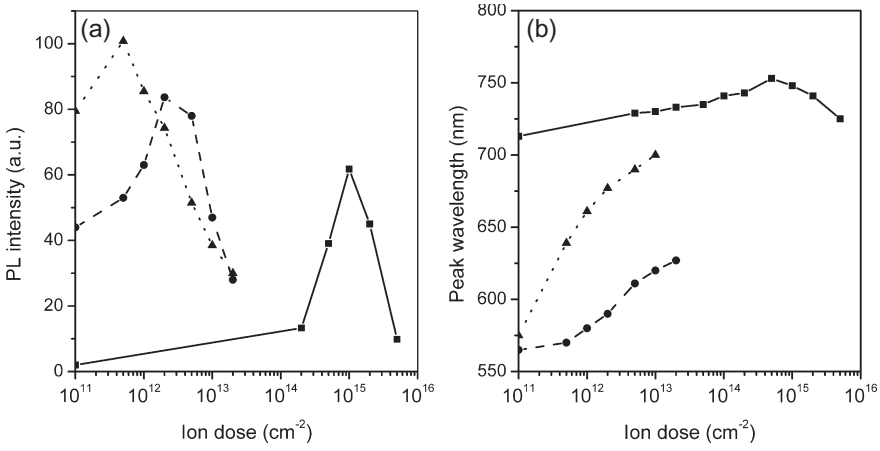

Figure 2. a) Measured PL intensity and b) peak-wavelength emission as a function of dose from Figure 1, for low- (0.02 Ω cm, solid line) and moderate-resistivity (0.3 Ω cm, dotted line and 3 Ω cm, dashed line) p-type silicon wafers.

Three different resistivity p-type silicon wafers were patterned with a focused beam of 2 MeV helium ions in a nuclear microprobe.[21,22] After irradiation, a contact was made to the back surface using Ga–In eutectic and copper wire. The wafers were anodized at a current density of 100 mA cm^{-2} for five minutes in a HF/ethanol/water electrolyte with a ratio 1:2:1, producing a porous layer several micrometers in thickness. The wafers were then washed in distilled water followed by ethanol and transferred immediately to a vacuum chamber. Figures 1,2 show PL images and plots of the PL intensity and peak-wavelength emission as a function of ion dose, respectively. The most notable feature of the low-resistivity wafer (0.02 Ω cm) is a factor-of-twenty increase in the intensity of red PL emission with increasing irradiation dose. In contrast, for moderate-resistivity wafers (0.3 Ω cm, 3 Ω cm) there is a red-shift up to 150 nm in the wavelength emitted from the irradiated areas with increasing dose, and a small peak in the intensity. It should be noted that the cracking effect observed in these films is a result of the drying process and can be reduced by freeze or supercritical drying.[23]

The mechanism underlying the large PL red-shift and intensity change with increasing ion dose from the different wafers can be explained in terms of the resulting increase in resistivity. Ion irradiation of silicon introduces lattice damage in the form of vacancy-interstitial pairs (Frenkel defects). For 2 MeV helium ions, the number of Frenkel defects is reasonably constant along the first six micrometers of the trajectory, then increases sharply towards the end of the penetration depth of the ions at ~7 μm.[20] Many factors influence the resulting hole concentration in p-type silicon that results from ion irradiation; defects may be stable or they may agglomerate into more stable divacancies and other vacancy- or impurity-related centers.[24–26] Electrically active defects form trap levels in the energy bandgap where charge carriers undergo

recombination through deep-level energy states, which reduces the hole density and increases the resistivity. The resistivity close to the surface of p-type silicon as a function of 2 MeV helium ion irradiation dose is plotted in Figure 3a, based on the measured values of defect production and trapping rates,[27] with changes in hole mobility with doping concentration taken into account. Of note is the rapid increase in resistivity above a certain dose threshold.

Figure 3b shows typical current-density versus applied-bias curves for p-type silicon undergoing anodization in a HF electrolyte,[5] the data exhibits characteristics similar to those of a Schottky diode. The curve at an ion-irradiated area, where the resistivity increases, is displaced to the right, compared with surrounding unirradiated material, resulting in a smaller local current density for a fixed applied bias. For example, a current density of 100 mA cm^{-2} passing through a low-resistivity wafer (0.02 Ω cm) would result in ~10 mA cm^{-2} passing through a region where ion irradiation has increased the resistivity to 3 Ω cm, as shown in Figure 3b. Ion irradiation thus alters both the resistivity of the near-surface region and also the hole current flowing through it, both of which effect porous silicon formation. In the case of n-type silicon,[28] ion irradiation has the opposite effect of lowering the electrochemical pore-formation potential, thus enhancing the likelihood of porous silicon formation in the irradiated regions.

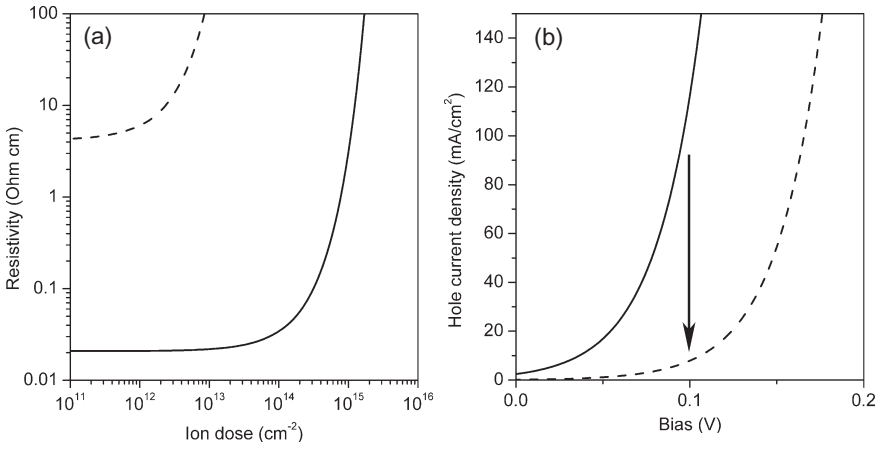

Figure 3. a) Calculated resistivity close to the surface of p-type silicon as a function of 2 MeV helium-ion dose, for low- (0.02 Ω cm, solid line) and moderate-resistivity (3 Ω cm, dashed line) p-type silicon wafers. b) Current density versus applied bias for low- and moderate-resistivity p-type silicon undergoing anodization in HF. The reduction in current density at an irradiated area is indicated by the arrow.

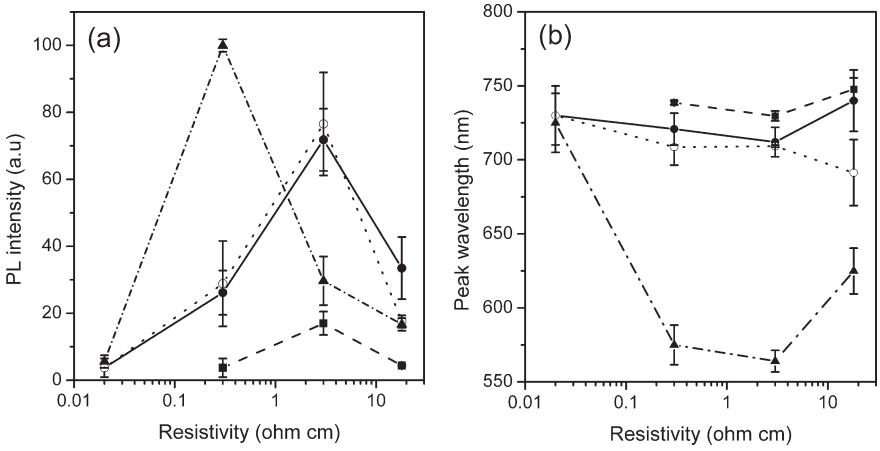

Figure 4. a) PL intensity and b) peak-wavelength measurements from bulk p-type wafers with resistivities of 0.02, 0.3, 3, and 20 Ω cm. The samples are anodized at four different current densities of 5 mA cm^{-2} (dashed line), 20 mA cm^{-2} (solid line), 50 mA cm^{-2} (dotted line), and 100 mA cm^{-2} (dotted–dashed line), each for 5 min under identical conditions.

Figure 4 shows a plot of PL intensity and peak-wavelength measurements as a function of the resistivity of unirradiated p-type bulk-silicon wafers. These exhibit similar trends to previous measurements,[5,29] and are interpreted using the quantum-confinement model;[7,30] pore-size classification is given by Lehmann [5]. The PL intensity is at a maximum and the emission wavelength at a minimum for wafers with a moderate resistivity of 0.1–10 Ω cm, where anodization produces a large fraction of microporous silicon, in which the remaining silicon islands typically have sizes of ≤2 nm. Quantum-confinement effects are expected to dominate when electrons are confined to a volume smaller than the exciton radius, equal to 4.9 nm for silicon. In this size regime, the energy bandgap is opened up from 1.1 eV to as large as 3 eV, allowing emission of visible PL over a wide range of wavelengths, depending on the pore size. In this resistivity range, a high current density produces PL emission wavelengths as short as 550 nm, which is progressively red-shifted with decreasing current density. Anodization of lower-/higher-resistivity wafers produces a significant fraction of mesoporous/macroporous silicon, where larger pore sizes result in weaker, red–orange PL emission.

The results in Figures 1,2 can now be understood within the context of ion-induced changes in resistivity and hole current. For unirradiated 0.02 Ω cm silicon, the PL intensity is faint at all current densities. The PL intensity from the irradiated regions peaks at a dose of 1×10^{15} cm^{-2}, where the resistivity is increased to within the range of 0.1–10 Ω cm; the region where formation of microporous silicon is favored. The full width at half maximum of the PL-intensity peak occurs over a narrow dose range, from 4×10^{14} to 3×10^{15} ions cm^{-1}, consis-

ADVANCED MATERIALS

tent with a rapidly increasing resistivity with dose in Figure 3a. The peak wavelength emission remains between 725 and 755 nm regardless of dose. At doses where moderate-resistivity silicon is formed, this is consistent with a significantly reduced current of 5–20 mA flowing through the irradiated area.

Irradiation of moderate-resistivity wafers reduces the current flowing through the irradiated region, resulting in PL emission which is red-shifted compared to the unirradiated background. The reduced current flow also initially increases the PL intensity, until the increased resistivity favors formation of macroporous silicon. Similar behavior is also observed with high-energy proton irradiation at doses typically twenty times larger than for helium ions, consistent with a comparable increase in resistivity.

Therefore there are two resistivity regimes in p-type silicon where porous silicon formation is affected in different ways by ion irradiation: for low-resistivity (~0.01 Ω cm) wafers irradiation primarily results in a large PL increase, whereas for moderate-resistivity (0.1–10 Ω cm) wafers irradiation primarily results in a large wavelength red-shift. A graphic demonstration of this different behavior is shown in Figures 5a,b. In low-resistivity silicon the irradiated dragon produces bright red PL compared with the faint unirradiated background. In

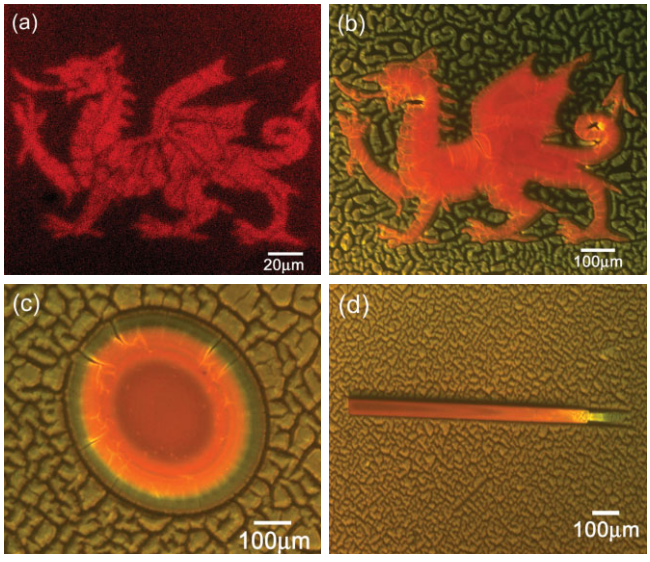

Figure 5. PL images of dragons formed by irradiating a) 0.02 Ω cm wafer with a dose of 1×10^{15} cm^{-2}, b) 3 Ω cm wafer with a dose of 5×10^{13} cm^{-2}. c) Concentric ring pattern formed by linearly increasing the dose from 5×10^{11} cm^{-2} at the outer edge to 1.2×10^{13} cm^{-2} at the centre. d) Colour bar showing a gradual wavelength red-shift as the dose increases from 2×10^{11} cm^{-2} at the right to 2×10^{13} cm^{-2} at the left.

moderate-resistivity silicon bright orange/red PL is produced from the dragon and the background produces green PL of similar intensity. The minimum resolvable line width of patterned areas using focused helium-ion irradiation in Figure 5a is about one micrometer. Figures 5c,d show examples whereby a range of doses have been irradiated along a continuous distribution in moderate-resistivity silicon, producing a gradual change in the PL emission wavelength. In Figure 5c, a circular region was irradiated with a dose which increased linearly towards the center, resulting in a gradual PL red-shift towards the center as the hole current is continuously reduced. The tapered region in Figure 5d was produced by a gradual increase in the irradiation dose from right to left, again resulting in a continuous red-shift.

Figure 6a shows a picture of the painting "The Ancient of Days" by William Blake (original in the British Museum, London). To demonstrate the versatility of our technique, we have reproduced a miniature version of the painting in porous silicon, shown in Figure 6b. The dose of each region is selected so that the PL emission from the porous silicon fits closely to the painting. The masculine body of the god, surrounded by a red, orange, and green aura, is depicted in orange and enhanced by the black outline produced by high-dose irradiation. The high spatial resolution of this technique has enabled us to discern the fine features on his face.

Figure 6. a) "The Ancient of Days" by William Blake (copyright the trustees of the British Museum; reproduced with permission). b) PL image of the painting produced by irradiation of 3 Ω cm resistivity silicon. The picture is irradiated with a dose of 5×10^{13} for black, 1×10^{13} for red, 5×10^{12} for orange, and 1×10^{12} cm^{-2} for yellow-green color.

In conclusion, we have demonstrated the ability to controllably red-shift the wavelength of the PL from patterned areas of p-type porous silicon over 150 nm in the visible spectrum, in which the intensity is also varied. This is achieved by pre-irradiating the silicon with a focused 2 MeV helium-ion beam, resulting in lattice damage which increases the resistivity and reduces the current flowing through the irradiated areas during subsequent etching. This gradual red-shift of the PL emission with dose can be explained by an increase in nanocrystal size as a result of the lower hole current through the damaged regions. Oxidation-related mechanisms may red-shift the PL emission from bulk wafers when exposed to air,[30] or blue-shift the emission when thermally[31] or chemically oxidized.[32] It is however difficult to envisage any such mechanism capable of producing widely differing emission wave-

lengths on the same wafer stored in vacuum, whereas such behavior is readily understandable using the quantum-confinement model. More work is needed to help understand the mechanism of the PL emission.

Experimental

The irradiation of p-type silicon with 2 MeV He was carried out using a single-ended accelerator. The desired pattern was fed into the IONSCAN software which then controlled the beam scanning. The dose at each region was controlled by the amount of time the beam dwelled at that region. After irradiation, the samples were cleaned with diluted HF (< 10 %) and electrical contact was made to the backside of the samples using In–Ga eutectic paint and copper wire. A thick layer of epoxy was applied to protect the electrical contact during etching. Subsequently, the samples were electrochemically etched in a solution of HF/H_2O/ethanol (1:1:2) at constant current density for 5 min. The current densities used varied from 5–100 mA cm^{-2}. The etched samples were then washed in a mixture of 1:1 ethanol and water solution and transferred immediately to a vacuum chamber. All characterizations using micro-PL spectroscopy were taken in vacuum at room temperature using a 405 nm diode laser. The laser light was focused onto the sample through a ME600 Nikon microscope with a 100x objective. The PL signals were detected using a charge-coupled device (CCD) Ocean Optics Spectrometer by means of an optical fiber. Most of the laser light was cut off from the PL signal with a 495 nm long-pass filter. All spectra have been corrected for system response. For PL imaging, the samples were excited with a UV lamp through a 400 nm filter and captured with a CCD camera.

Received: June 3, 2005
Final version: September 24, 2005
Published online: November 21, 2005

[1] Z. H. Lu, D. J. Lockwood, J.-M. Baribeau, *Nature* **1995**, *378*, 258.
[2] L. Pavesi, L. Dal Negro, C. Mazzoleni, G. Franzo, F. Priolo, *Nature* **2000**, *408*, 440.
[3] H. Rong, R. Jones, A. Liu, O. Cohen, D. Hak, A. Fang, M. Paniccia, *Nature* **2005**, *433*, 725.
[4] L. T. Canham, *Nature* **2000**, *408*, 411.
[5] V. Lehmann, in *Electrochemistry of Silicon*, Wiley-VCH, Weinheim, Germany **2002**.
[6] L. T. Canham, *Appl. Phys. Lett.* **1990**, *57*, 1046.
[7] A. G. Cullis, L. T. Canham, *Nature* **1991**, *353*, 335.
[8] M. J. Sailor, E. J. Lee, *Adv. Mater.* **1997**, *9*, 783.
[9] S. Ossicini, L. Pavesi, F. Priolo, in *Light Emitting Silicon for Microphotonics*, Vol. 194, Springer-Verlag, Berlin, Germany **2003**, pp. 75–122.
[10] K. D. Hirschman, L. Tsybeskov, S. P. Duttagupta, P. M. Fauchet, *Nature* **1996**, *384*, 338.
[11] A. Briner, R. B. Wehrspohn, U. M. Gösele, K. Busch, *Adv. Mater.* **2001**, *13*, 377.
[12] V. V. Doan, M. J. Sailor, *Science* **1992**, *256*, 1791.
[13] S. P. Duttagupta, C. Peng, P. M. Fauchet, S. K. Kurinec, T. N. Blanton, *J. Vac. Sci. Technol. B* **1995**, *13*, 1230.
[14] M. Rocchia, S. Borini, A. M. Rossi, L. Boarino, G. Amato, *Adv. Mater.* **2003**, *15*, 1465.
[15] D. J. Sirbuly, G. M. Lowman, B. Scott, G. D. Stucky, S. K. Buratto, *Adv. Mater.* **2003**, *15*, 149.
[16] X. M. Bao, H. Q. Yang, F. Yan, *J. Appl. Phys.* **1993**, *79*, 1320.
[17] S. Chattopadhyay, P. W. Bohn, *J. Appl. Phys.* **2004**, *96*, 6888.
[18] E. J. Teo, D. Mangaiyarkarasi, M. B. H. Breese, A. A. Bettiol, D. J. Blackwood, *Appl. Phys. Lett.* **2004**, *85*, 4370.
[19] L. Pavesi, G. Giebel, F. Ziglio, G. Mariotto, F. Priolo, S. U. Campisano, C. Spinella, *Appl. Phys. Lett.* **1994**, *65*, 2182.
[20] J. F. Ziegler, J. P. Biersack, U. Littmark, in *The Stopping and Range of Ions in Solids*, Pergamon Press, New York **1985**.
[21] M. B. H. Breese, D. N. Jamieson, P. J. C. King, in *Materials Analysis using a Nuclear Microprobe*, Wiley, New York **1996**.
[22] J. A. van Kan, A. A. Bettiol, F. Watt, *Appl. Phys. Lett.* **2003**, *83*, 1629.
[23] L. T. Canham, A. G. Cullis, C. Pickering, O. D. Dosserm, T. I. Cox, T. P. Lynch, *Nature* **1994**, *368*, 133.
[24] B. G. Svensson, B. Mohadjeri, A. Hallen, J. H. Svensson, J. W. Corbett, *Phys. Rev. B* **1991**, *43*, 2292.
[25] B. G. Svensson, C. Jagadish, A. Hallen, J. Lalita, *Nucl. Instrum. Methods Phys. Res. Sect. B* **1995**, *106*, 183.
[26] A. Hallen, N. Keskitalo, F. Masszi, V. Nagi, *J. Appl. Phys.* **1996**, *79*, 3906.
[27] M. Yamaguchi, S. J. Taylor, Yang, S. Matsuda, O. Kawasaki, T. Hisamatsu, *J. Appl. Phys.* **1996**, *80*, 4916.
[28] P. Schmuki, L. E. Erickson, D. J. Lockwood, *Phys. Rev. Lett.* **1998**, *80*, 4060.
[29] Z. Gaburro, H. You, D. Babic, *J. Appl. Phys.* **1998**, *84*, 6345.
[30] M. V. Wolkin, J. Jorne, P. M. Fauchet, G. Allan, C. Delerue, *Phys. Rev. Lett.* **1999**, *82*, 197.
[31] L. Tsybeskov, J. V. Vandyshev, P. M. Fauchet, *Phys. Rev. B* **1994**, *49*, 7821.
[32] K. Y. Suh., Y. S. Kim, S. Y. Park, H. H. Lee, *J. Electrochem. Soc.* **2001**, *148*, C439.

DOI: 10.1002/adma.200501455

Self-Assembly Combined with Photopolymerization for the Fabrication of Fluorescence "Turn-On" Vesicle Sensors with Reversible "On–Off" Switching Properties**

By *Guangyu Ma*, *Astrid M. Müller*, *Christopher J. Bardeen*, and *Quan Cheng**

There is considerable interest in the development of self-amplifying polymeric materials that render direct fluorescence measurements of analytes by means of detecting changes of fluorescence intensity, wavelength, or lifetime.[1–3] Swager and co-workers have examined a series of conjugated polymers as the sensing material for a variety of molecular targets.[2,4–6] In these "smart" materials, the excited states (excitons) propagating along the conjugated backbone are quenched on encounter-

[*] Prof. Q. Cheng, G. Ma, Dr. A. M. Müller, Prof. C. J. Bardeen
Department of Chemistry, University of California
Riverside, CA 92521 (USA)
E-mail: quan.cheng@ucr.edu

[**] Q. C. acknowledges the support of the UC Riverside and the Eli Lilly analytical chemistry grant. C. J. B. acknowledges the support from NSF grant CHE-0517095. Supporting Information, including details of experimental procedure and characterization, is available online from Wiley InterScience or from the author.